

## Electroshock plastic constitutive modelling of high strength aluminum alloy based on GA-BP neural network

SONG Yanli<sup>1,a\*</sup>, XU Hainan<sup>1,b</sup>, CHEN Long<sup>1,c</sup>, LU Jue<sup>1,d</sup> and HUA Lin<sup>1,e\*</sup>

<sup>1</sup>Hubei Key Laboratory of Advanced Technology for Automotive Components, Wuhan University of Technology, Wuhan 430070, China

<sup>a</sup>ylsong@whut.edu.cn, <sup>b</sup>xhn0801@whut.edu.cn, <sup>c</sup>335194@whut.edu.cn, <sup>d</sup>lujue@whut.edu.cn, <sup>e</sup>hualin@whut.edu.cn

**Keywords:** 7075 Aluminum Alloy, Genetic Algorithm, BP Neural Network, Electroshock Plastic Constitutive Model, Electrically-Assisted Forming

**Abstract.** Electrically-assisted forming is an effective way to improve the difficult-to-form materials. On basis of electro- and magneto- plastic effects, our team put forward a novel electroshock treatment (EST) process, which can not only improve the formability of the material but also improve the service performance of the formed parts. However, electrically-assisted forming involves nonlinear deformation with multi-physics coupling, the microstructural evolution and plastic mechanical response of materials under the coupling of electric current field and stress field are highly intricate, posing significant challenges in predicting macroscopic deformation behavior. The study of the characterization and precise control of plastic deformation's constitutive relation is therefore highly significant. In this work, the stress-strain curves of AA7075 under, different current densities, periods and power duration are obtained by means of the pulse electric current assisted tension test, and the intelligent prediction of the electroshock plastic constitutive relationship of AA7075 is realized based on the Genetic Algorithm (GA) optimized Back Propagation (BP) (GA-BP) neural network. The results show that the proposed algorithm can reduce the input parameters of the constitutive model to current, temperature and strain, and improve the computational efficiency. GA is used to optimize the initial weight and threshold of BP neural network, and the best hidden node number was selected as 12 by error verification to train the network. Compared with the traditional BP neural network, the neural network optimized by GA has higher accuracy, and in the plastic deformation stage, the coefficient of determination  $R^2$  between the predicted results and the experimental results is basically 99%, which is about 20% higher than that of the BP neural network. At the same time, it solves the data fluctuation in the long-term prediction due to the standard of satisfying the error in the prediction.

### Introduction

In recent years, the application of electrically-assisted forming in improving the formability of metal materials has received widespread attention, since it can improve the plasticity and forming performance of the material and reduce flow stress and springback [1]. During the electrically-assisted forming process, the material is subject to the coupling effect of multiple physical fields, and its macroscopic mechanical response and microstructure evolution are very complex. Hao et al. [2] studied the effect of extremely low frequency electric pulse on the mechanical properties of AA7075-T6, and found that the tension strength of AA7075-T6 was reduced by the pulse electric current assisted tension, the elongation of the specimen after fracture can be increased by 32.3%, and a linear relationship can be established between the current density, duration and the stress drop. Conrad et al. [3] explored the influence of an electron wind on each of the parameters in the equation for the thermally-activated motion of dislocations, and found that the pre-exponential impact was the greatest and the derived electron wind push coefficient was one or more orders of



magnitude larger than the value normally accepted for the electron drag coefficient. Ross et al. [4] studied the material property response of Ti-6Al-4V alloy under the action of electric current and the electromigration theory of metals. They applied the EAF process to the forming process and found that the electric current can be used at lower temperatures. Reduce the deformation resistance of the material, improve the formability of the metal during deformation and reduce springback after deformation.

Traditionally, material constitutive equations are established by multiple linear regression analysis of experimental results. However, many factors affecting flow stress are highly nonlinear, which makes the establishment of theoretical models difficult and easy to deviate from the actual situation. There are three main methods for establishing constitutive models: phenomenological models fitted by empirical formulas, models based on physical internal variables and statistical models based on test data. The test data statistical model has fast operation speed and high accuracy. Therefore, the neural network was used to establish the constitutive relationship of the material, and has been widely used. Commonly used intelligent algorithms are usually predicted by neural networks such as Back Propagation, Artificial, and Elman. Wan et al. [5] used Back Propagation (BP) neural network to establish a Zr-4 alloy constitutive model. The correlation coefficient is 0.9981, the average absolute relative error is 4.497, and 93.75% of the data points deviate from the predicted value within 10%. Yu et al. [6] established an Artificial neural network constitutive model of Zr based the bulk metallic glass composites based on Genetic Algorithm (GA) and particle swarm optimization (PSO). The study found that compared with the traditional constitutive model, the constitutive model established through neural network is more accurate and more suitable for (Zr55Cu30Al10Ni5)94Ta6. Neural network is a complex nonlinear system with high adaptability, self-learning and fault tolerance capabilities. When it is applied to complex nonlinear prediction, its effect is better. The GA has the ability to quickly seek optimization.

A novel electroshock plasticizing forming process has been proposed by our team, which can not only improve the formability of the material but also improve the service performance of the formed parts [2]. However, there is still a lack of constitutive equations to quantitatively describe its periodic zigzag stress-strain behavior. This paper uses GA to optimize the weights and thresholds of BP neural network, and establishes a constitutive relationship prediction model of AA7075-T6 under electroshock based on GA-BP neural network. This model can be used to predict AA7075-T6 rheological behavior of alloys under electroshock treatment (EST).

### Experimental process and mechanical behavior analysis

**Experimental Materials.** This paper uses AA7075-T6 as the test material, and the specimen thickness is 1.6mm. Its nominal chemical composition is shown in Table 1. The tension specimen required for the pulse electric current assisted tension test was prepared by laser cutting along the rolling direction of the sheet, and then the flash on the edge of the specimen was polished with 800-grit and 1500-grit sandpaper. The specific dimensional drawings and physical pictures are as follows as shown in Fig. 1. In order to facilitate the power supply, both ends of the specimen were additionally processed into terminals. The specimen and cable are reliably connected using bolts and nuts.

*Table 1. Nominal chemical compositions of AA7075-T6 sheets (wt. %).*

| Si   | Fe   | Cu   | Mn    | Mg   | Cr   | Zn   | Ti    | Al   |
|------|------|------|-------|------|------|------|-------|------|
| 0.40 | 0.35 | 1.52 | 0.092 | 2.66 | 0.22 | 5.28 | 0.029 | Bal. |

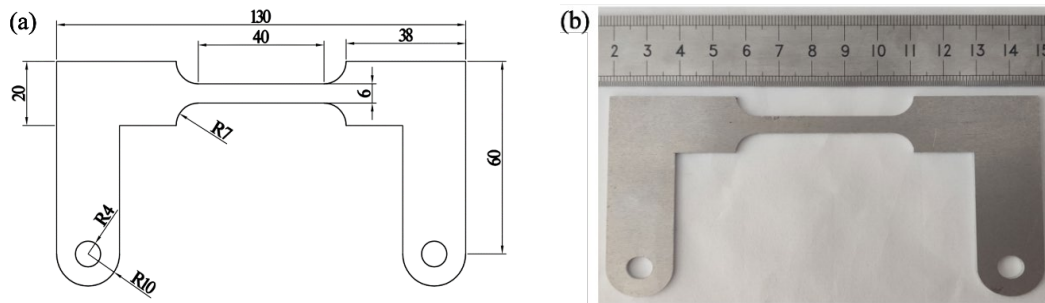


Fig. 1. The pulse electric current assisted quasi-static unidirectional tension test specimens: (a) dimensional drawing; (b) photograph (Unit of length: mm).

Experimental method. The physical diagram and schematic diagram of the pulse electric current assisted tension equipment are shown in Fig. 2. It consists of a DC power supply, the electronic universal tension testing machine and a Fotric 226 infrared thermometer. The electronic universal tension testing machine is a CMT of the SANS MTS brand. Model -5205, the maximum test force is 200kN, the load accuracy is  $\pm 0.5\%$ , and the data sampling interval is 0.01s. During the pulse electric current assisted tension test, electric pulses and quasi-static tension loads are applied to the specimen simultaneously. An insulation conversion head is installed between the chuck and chuck base of the testing machine to ensure sufficient insulation between the universal testing machine and the tension specimen. At the same time, the temperature of the specimen surface is measured with an infrared thermometer, and a layer of black paint is sprayed on the specimen surface to increase the energy emissivity, thereby improving measurement accuracy.

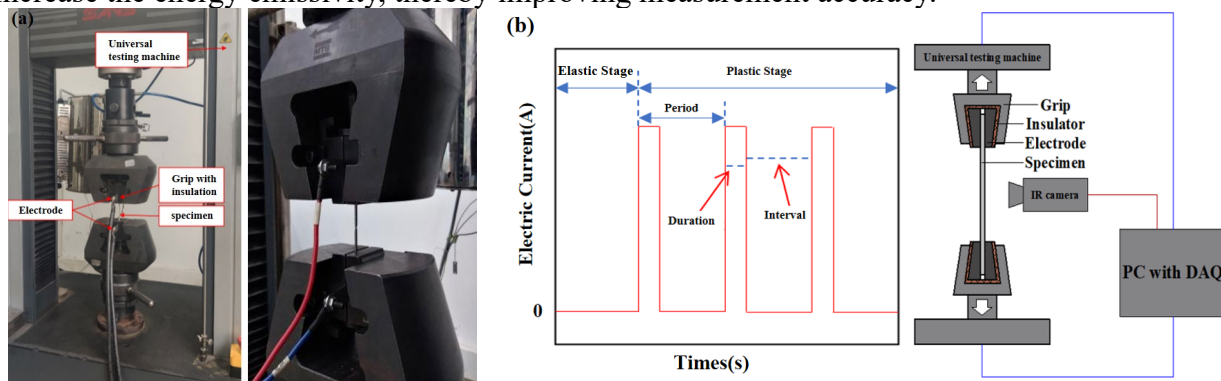


Fig. 2. The pulse electric current assisted quasi-static unidirectional tension platform: (a) schematic diagram; (b) photograph.

The pulse electric current assisted quasi-static unidirectional tension test of AA7075-T6 was carried out with different current density (J), pulse duration (td) and pulse period ( $\omega$ ) as process parameters, and the pulse electric current waveform is a unidirectional wave with constant current density and pulse period. Each set of tests starts to energize after the material enters plastic deformation.

The current density was selected as 50 A/mm<sup>2</sup> and 60 A/mm<sup>2</sup>, the pulse time is 1s, 3s, and the pulse period is 30 s, 40 s. Among them, the current density J is the ratio of the current value output by the pulse power supply to the cross-section of the specimen gauge section, and the unit is A/mm<sup>2</sup>. In the pulse electric current assisted quasi-static unidirectional tension test, the medium speed was maintained at 2.4 mm/min. The relationship between the specimen strain rate and the displacement speed of the tension testing machine beam is:

$$\dot{\epsilon} = \frac{v}{60L_c} \quad (1)$$

where  $\dot{\epsilon}$  is the strain rate of the specimen ( $s^{-1}$ );  $V$  is the beam displacement speed of the tension testing machine mm/min;  $L_C$  is the gauge length.

During the experiment, the microcomputer processing system automatically collects, calculates and corrects the experimental data, and outputs the flow stress data under different current densities, different pulse periods and different pulse durations. At the same time, the infrared thermometer records the surface stress of the specimen temperature.

Analysis of electroshock plasticizing mechanical behavior. Fig. 3. shows the true stress-strain curves of AA7075-T6 under tension effects of  $50A/mm^2-3s-40s$ ,  $60A/mm^2-1s-30s$ , and  $60A/mm^2-3s-40s$ . During the plastic deformation stage, after the current flows during the pulse duration, the stress value of the aluminum alloy material will suddenly drop. When the current flows and enters the pulse interval, the stress value rises in a slope, then enters the strengthening stage, completing a local stress-strain curve, and then continues this cycle after the arrival of the second electroshock until the specimen breaks. It can be seen from the blue curve and black curve in Fig. 3 that under the same pulse period and different current densities, the stress drop value after each electrical pulse shock increases with the increase of current density. While for the blue curve and the red curve, it can be seen that under the same current density and different pulse periods, the longer the current duration, the more obvious the stress drop, and the overall trend of stress is downward in a longer duration.

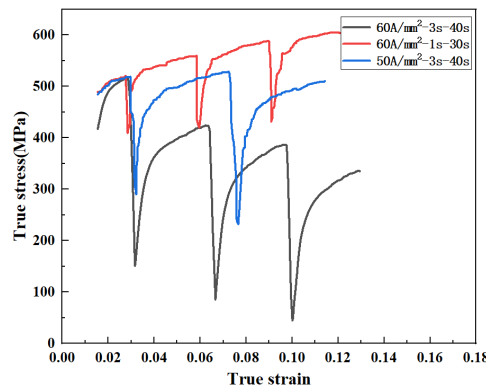


Fig. 3. The true stress-strain curves of AA7075-T6 under three different states of the pulse electric current assisted quasi-static unidirectional tension.

**Neural network constitutive model based on neural network**

BP neural network theory. The nonlinear mapping relationship of the BP neural network model is superior to the linear relationship of the multiple linear regression model in processing variables, and is widely used in various complex system analysis, especially in aspects such as simulation, fitting, and prediction that are difficult to quantitatively analyze [7]. Its structure is shown in Fig. 4.

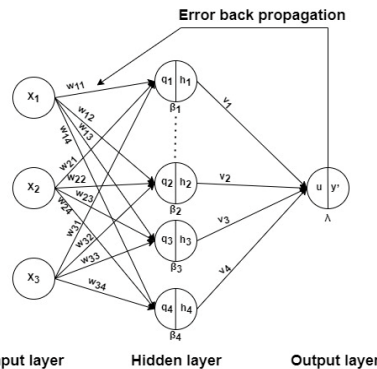


Fig. 4. BP neural network structure.

In this work, the strain, temperature and current obtained during the pulse electric current assisted quasi-static unidirectional tension test of AA7075-T6 are used as input, and the stress is used as output. Therefore, the number of neurons in the input layer is 3, and the number of neurons in the output layer 1. First, normalize the data [8]:

$$X' = \frac{x - x_{\min}}{x_{\max} - x_{\min}} \quad (2)$$

where  $x'$  is the normalized data;  $x$  is the original input data,  $x_{\max}$  and  $x_{\min}$  respectively correspond to the maximum and minimum values of the original input data.

Genetic algorithm. GA is a stochastic global search optimization method that simulates phenomena such as replication, crossover, and mutation that occur in natural selection and inheritance, allowing the population to evolve to better and better areas in the search space [9], thereby obtaining high-quality solutions to the problem. The steps of the GA are shown in Table 2:

*Table 2. GA steps.*

| Number | Name       | Definition  | Methods  |
|--------|------------|---|--|
| 1      | Encoding   | GA mapping in space and mapping traits to genes.  | Encoding method: number encoding.                                  |
| 2      | Population | Randomly generate n initial individuals to form a population.   | /  |
| 3      | Fitness    | The higher the fitness, the better the individual is.   | /  |
| 4      | Selection  | Select individuals with higher fitness to enter the next generation.  | Selection method: roulette.  |
| 5      | Crossover  | Select individuals from two parents and exchange part of the genes of the parents to produce new offspring. | Crossover method: the two-point crossover, the probability is 0.8. |
| 6      | Mutation   | One or several genes on a chromosome mutate, forming new chromosomes.                                       | The probability is 0.01.   |

According to the empirical formula, the larger the population size, the better is not generally selected. Although the search ability is stronger if the size is too large, the algorithm time will be too long, and the search ability of smaller scales is limited. Considering the complexity of the problem, through experience and experiments, the earliest Determine and select the initial population size as 50, and set the parameters of the GA as follows:

*Table 3. The setting of experimental parameters.*

| Parameter settings    | Value |
|-----------------------|-------|
| Population size       | 50    |
| Crossover probability | 0.8   |
| Mutation probability  | 0.01  |
| Number of iterations  | 50    |

### Analysis of prediction results of constitutive model

The prediction effect of the constitutive model of the plastic deformation stage of the AA7075-T6 obtained by the BP neural network is shown in Fig. 5, where the coefficient of determination  $R^2$  in the Fig. (a), (b), (c) is 0.75, 0.85 and 0.84. From a mathematical point of view, the BP algorithm is a local search method. When solving the global extreme value of some complex nonlinear functions, the algorithm may fall into a local minimum, causing training to fail. And the training of neural network is the process of solving the optimal weights and biases. Different initial weights and biases have a great impact on the training of the network. It is necessary to try different initial values many times to obtain the optimal network, so the task is heavy and causes greater randomness to the results. And because the BP neural network prediction stops network training based on whether the target error meets the conditions, this also leads to the fact that although the BP neural network prediction result is within the error range, it may fluctuate up and down, leading to prediction of the actual result. Trend generates errors [10], Fig. 5(d) shows a partial enlargement of Fig. 5(c).

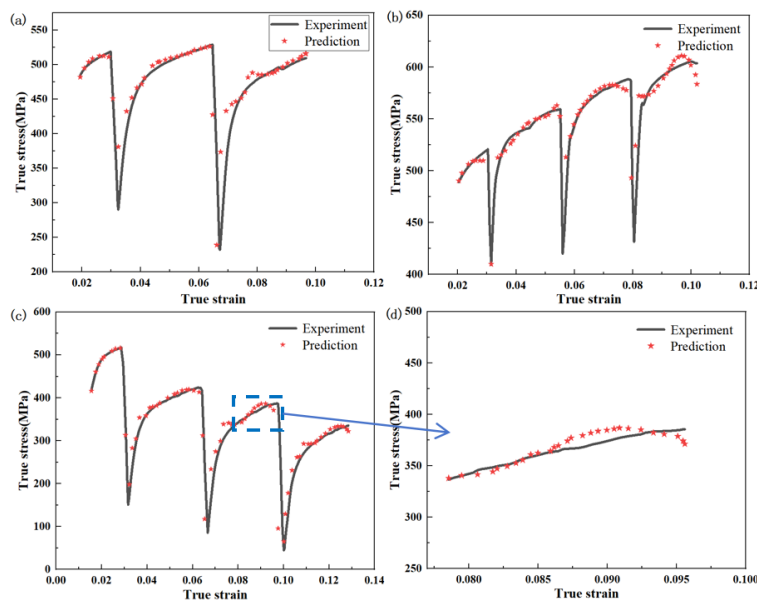


Fig. 5. The true stress-strain of AA7075-T6 based on BP model under various conditions: (a)  $50A/mm^2-3s-40s$ , (b)  $60A/mm^2-1s-30s$ , (c)  $60A/mm^2-3s-40s$ , (d) partial enlargement of c.

After optimizing the BP neural network using GA, the prediction effect of the plastic deformation stage of the AA7075-T6 is obtained, as shown in Fig. 6, and the prediction accuracy of the optimized neural network reaches 99%, and the fluctuations of the predicted values are also in line with the actual trend.

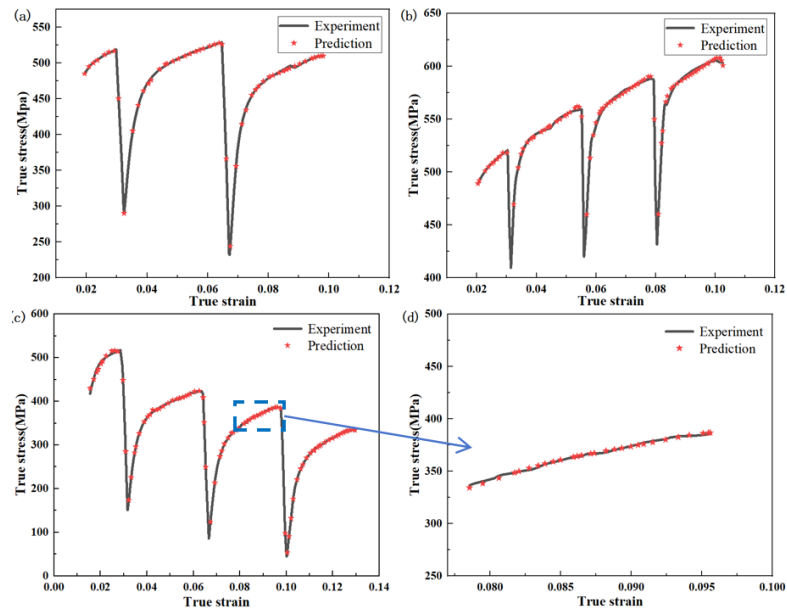


Fig. 6. The true stress-true strain of AA7075-T6 based on GA-BP model under various conditions: (a) 50A/mm<sup>2</sup>-3s-40s, (b) 60A/mm<sup>2</sup>-1s-30s, (c) 60A/mm<sup>2</sup>-3s-40s, (d) partial enlargement of c.

The Fig. 7 is the error diagram between the predicted results and the actual results. It can be seen from the figure that the error fluctuations are small, and the maximum error does not exceed 25 MPa. The larger error fluctuations exist in the turning point of stress decline and rise. Because the number of specimens here is small, and the neural network is more sensitive to small changes in specimen data, the prediction results will have slightly larger fluctuations. The fluctuations at the end and front end in Fig. 7(b) and c are due to sampling, due to sudden small changes in the data detected by the microcomputer. Besides, the setting neural network threshold is too large, resulting in large fluctuations. Subsequent improvement work needs to use a greater frequency in the turning point of stress decline and rise during data sampling to obtain more data, and at the same time reduce the threshold of the neural network, thereby reducing the error.

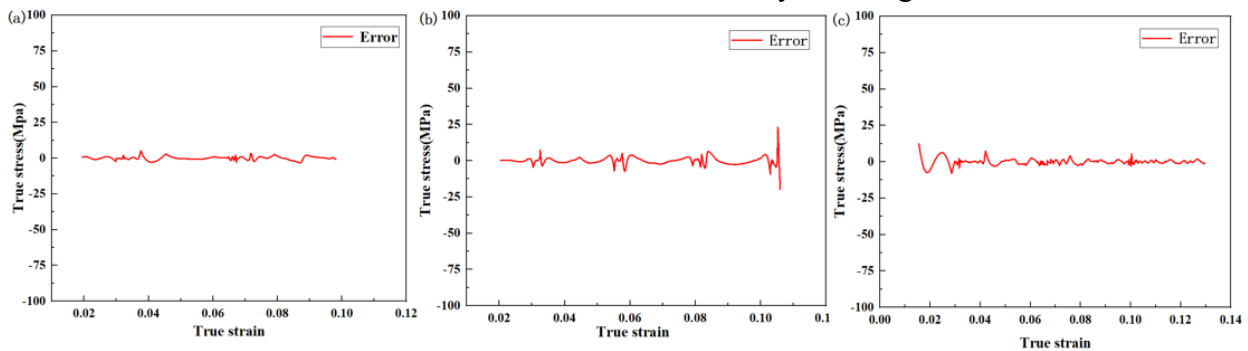


Fig. 7. The true stress- strain prediction error of AA7075-T6 based on GA-BP: (a) 50A/mm<sup>2</sup>-3s-40s, (b) 60A/mm<sup>2</sup>-1s-30s, (c) 60A/mm<sup>2</sup>-3s-40s.

### Conclusions

This paper uses a GA to optimize the BP neural network to predict the constitutive relationship of AA7075-T6 during the pulse electric current assisted quasi-static unidirectional tension:

(1) Build a BP neural network model to predict constitutive relationships. Experimental data show that the fitting accuracy of BP neural network does not meet the requirements, and the predicted data trend is inconsistent with the actual situation. Therefore, in view of the above situation, the GA is used to optimize the initial weight threshold of the BP neural network to obtain

the best prediction results.

(2) Using the global search capability of the GA, the optimal initial weight is found. The optimized neural network has greatly improved the prediction accuracy. The determination coefficient  $R^2$  of its prediction results has reached 99%. The error ranges of the three prediction results are all within 25MPa, which meets the prediction requirements. Compared with the BP neural network The prediction accuracy is increased by about 20%, and the inaccuracy of the BP neural network in predicting trends is improved.

(3) It is found that the neural network prediction has large error fluctuations, which are more obvious when the stress decreases and rises suddenly. The reason is that there is less sampling data at the fluctuation point and the threshold setting is too large. The improvement measure is to increase the fluctuation. Larger sampling frequency and set smaller threshold.

### Acknowledgements

This work was financially supported by the National Key Research and Development Project of China (Grand No. 2020YFA0714900), and the National Natural Science Foundation of China (51975440).

### References

- [1] S. Wang, A. Xiao, Y. Lin, Effect of induced pulse current on mechanical properties and microstructure of rolled 5052 aluminum alloy, *J. Materials Characterization*. 185 (2022) 111757. <https://doi.org/10.1016/j.matchar.2022.111757>
- [2] Y. Song, C. Hao, Effect of Extremely Low Frequency Pulse Current Treatment on the Mechanical Properties of Al-Zn-Mg-Cu Aluminum Alloy, *J. Mech. Eng.* 58 (2022) 68-77. <https://doi.org/10.3901/JME.2022.10.068>
- [3] H. Conrad, Thermally activated plastic flow of metals and ceramics with an electric field or current, *Mater. Sci. Eng. A* 322 (2002) 100-107. [https://doi.org/10.1016/S0921-5093\(01\)01122-4](https://doi.org/10.1016/S0921-5093(01)01122-4)
- [4] C.D. Ross, T.J. Kronenberger, J.T. Roth, Effect of DC on the formability of Ti-6Al-4V, *J. Eng. Mater. Tech.-Transactions of the ASME* 131 (2009). <https://doi.org/10.1115/1.3078307>
- [5] P. Wan, H. Zou, K. Wang, Research on hot deformation behavior of Zr-4 alloy based on PSO-BP artificial neural network, *J. Alloy. Compd.* 826 (2020) 154047. <https://doi.org/10.1016/j.jallcom.2020.154047>
- [6] G. Yu, X. Bao, X. Xu, Constitutive modeling of Ta-rich particle reinforced Zr-based bulk metallic composites in the supercooled liquid region by using evolutionary artificial neural network, *J. Alloy. Compd.* 938 (2023) 168488. <https://doi.org/10.1016/j.jallcom.2022.168488>
- [7] R. Chen, J. Song, M. Xu, Prediction of the corrosion depth of oil well cement corroded by carbon dioxide using GA-BP neural network, *Constr. Build. Mater.* 394 (2023) 132127. <https://doi.org/10.1016/j.conbuildmat.2023.132127>
- [8] J. Shi, J. Wang, D.D. Macdonald, Prediction of primary water stress corrosion crack growth rates in Alloy 600 using artificial neural networks, *Corros. Sci.* 92 (2015) 217-227. <https://doi.org/10.1016/j.corsci.2014.12.007>
- [9] K.G. Srinivasa, K.R. Venugopal, L.M. Patnaik, A self-adaptive migration model genetic algorithm for data mining applications, *Inform. Sci.* 177 (2007) 4295-4313. <https://doi.org/10.1016/j.ins.2007.05.008>
- [10] Y. Zhou, S. Li, BP neural network modeling with sensitivity analysis on monotonicity based Spearman coefficient, *Chemometr. Intell. Lab.* 200 (2020) 103977. <https://doi.org/10.1016/j.chemolab.2020.103977>